

Article

Economic and Experimental Assessment of KCOOH Hybrid Liquid Desiccant-Vapor Compression System

Kashish Kumar *  and Alok Singh

Department of Mechanical Engineering, Maulana Azad National Institute of Technology, Bhopal 462003, India

* Correspondence: kash251191@gmail.com

Abstract: A liquid desiccant dehumidification cooling system is a promising, energy-saving, high-efficiency, environmentally friendly technology that maintains thermal comfort effectively indoors by utilizing renewable energy sources or waste heat to enhance system efficiency. In this research, a small-scale (6 kW cooling capacity) hybrid liquid desiccant air-conditioning system (HLDAC) is proposed to evaluate the dehumidification performance of a non-corrosive potassium formate (KCOOH) solution. For this, four input parameters, namely, inlet air flow rate, inlet desiccant temperature, inlet desiccant concentration, and inlet specific air humidity, were selected. Moreover, the different combinations of experiments were designed by employing response surface methodology (RSM) to evaluate the dehumidification performance parameters, namely, dehumidifier latent heat load, coefficient of performance of hybrid system, and moisture removal rate (MRR). Further, a comparative performance analysis between the hybrid system and a standalone vapor compression system (VCS) unit was carried out. The result showed a remarkable increase in coefficient of performance, which was observed at about 28.48% over the standalone VCS unit. Furthermore, the economic assessment of the proposed hybrid system is presented in this paper. Finally, from the economic analysis, it was concluded that the hybrid system had a payback time of 2.65 years compared to the VCS unit.

Keywords: hybrid energy-efficient system; vapor compression refrigeration; dehumidification performance; energy conservation; payback period



Citation: Kumar, K.; Singh, A. Economic and Experimental Assessment of KCOOH Hybrid Liquid Desiccant-Vapor Compression System. *Sustainability* **2022**, *14*, 15917. <https://doi.org/10.3390/su142315917>

Academic Editors: Yuehong Su, Jae-Weon Jeong, Jingyu Cao, Devrim Aydin, Michele Bottarelli and Carlos Jimenez-Bescos

Received: 29 September 2022

Accepted: 8 November 2022

Published: 29 November 2022

Publisher's Note: MDPI stays neutral with regard to jurisdictional claims in published maps and institutional affiliations.



Copyright: © 2022 by the authors. Licensee MDPI, Basel, Switzerland. This article is an open access article distributed under the terms and conditions of the Creative Commons Attribution (CC BY) license (<https://creativecommons.org/licenses/by/4.0/>).

1. Introduction

Air conditioning (AC) is acknowledged as a crucial means of upgrading the comfort level and living environment for humans, as people spend up to 70–90% of their lives indoors. The parameters for better indoor air quality include airborne pollutants, ventilation, thermal comfort, humidity, acoustic conditions, and other variables [1]. Usually, thermal comfort and humidity are the two important factors that are regulated by AC systems. It is anticipated that, in the future, AC systems will need more energy to provide a comfortable indoor environment due to the rising demand for a high quality of life [2]. Hence, improving the effectiveness of AC systems is consequently a prominent topic of discussion. Moreover, worries about global warming and other forms of environmental degradation have increased the demand for buildings to reduce their cooling and air conditioning energy use [3]. In recent years, the vapor compression system (VCS) has gained popularity due to its compact size, the ability to handle sensible heat load effectively with high heat transfer, and operation convenience [4]. However, it has always been criticized for its significant dependence on electricity, inadequate humidity control, and ineffective handling of latent heat load as supercooling is done below its dew point temperature and afterward reheating is done to the desired indoor condition, which results in significant energy consumption. In addition, health issues might arise because the coil surface in the VCS can act as a fertile source for microorganisms due to the condensed water. Therefore, a persistent effort has been made by the researchers to search for better alternative AC systems.

The liquid desiccant dehumidification system (LDDS) is gaining popularity for the dehumidification of indoor air as it requires less energy since liquid desiccant collects moisture straight from the air. Therefore, it may be utilized as an efficient supplement to conventional VCS as it has better humidity control with an effective approach towards latent heat load and has the possibility of being powered by renewable or low-grade energy. With a new hybrid technology, the benefits of both liquid desiccant dehumidification and VCS can be used together. Extensive research has been carried out for hybrid liquid desiccant air-conditioning (HLDAC) aiming to improve the effectiveness and performance of traditional AC systems. Mohammad et al. [5] studied different types of hybrid liquid desiccant air-conditioning (LDAC) systems based on the VCS and concluded that this novel technology has the capacity to remove air moisture in hot and humid regions with energy-saving potential as the liquid desiccant can be regenerated with waste heat or renewable energy. Additionally, the VCS is compact in size and thus enhances its coefficient of performance (COP). Jain et al. [6] investigated an electric power-driven hybrid LDAC system and compiled experimental data on a packed bed dehumidifier with three desiccants (i.e., calcium chloride (CaCl_2), lithium chloride (LiCl), and triethylene glycol (TEG)), and empirical correlations were developed. Dai et al. [7] experimentally investigated a hybrid LDAC system comprised of a VCS, a liquid desiccant system, and an evaporative cooler, and the COP was found to be 1.513, 1.862, and 1.745 while using VCS, VCS + desiccant dehumidification, and VCS + desiccant dehumidification + evaporative cooling, respectively. Al-Farayedhi et al. [8] suggested a system consisting of a packed-bed dehumidifier with a five-ton capacity VCS while employing CaCl_2 as liquid desiccant, and results revealed that temperature of the air was reduced from 48 to 38 °C and the value of outlet-to-inlet absolute humidity was found to be 0.6. The $\text{COP}_{\text{hybrid}}$ was calculated in three different regeneration modes: 1.164 (while heating desiccant), 1.616 (while heating air), and 1.4221 (while heating both air and desiccant), and the COP of the standalone VCS was 0.989. Lee et al. [9] experimentally investigated a proposed heat pump driven hybrid LDAC system in which the heat pump accommodates the heating and cooling demands of liquid desiccant. The result was that COP was found to be 2.26 in the summer with 7.45 kW cooling capacity and the COP in the winter was found to be 2.51 with 5.075 kW. Guan et al. [10] discussed the performance of an on-site novel hybrid LDAC system in an industrial factory. The COP of the system was 3.6, which was enhanced by 25.6% and saved about 23.3% energy. This is achieved as this proposed system needs chilled water without reheating because of the use of the dehumidifier. Mansuriya et al. [11] performed an experimental study on a small-scale 5 kW hybrid LDAC system in which a VCS unit is employed to enhance the $\text{COP}_{\text{hybrid}}$ by 27.54% and the share of total latent heat load (LHL) of the system, 54.93%, is shared by the dehumidifier unit with a payback time of four years. In another study [12], they performed a thermo-economic assessment of the proposed system with COP and annual cost as objectives. The investigation concluded that the COP was improved by up to 68.4% compared to the standalone COP, and the payback duration was found to be 1.54.

The key element of the LDDS is a liquid desiccant that has a significant ability to absorb moisture. The liquid desiccants are chemicals that have hygroscopic characteristics that absorb atmospheric moisture (i.e., dehumidifying air) and decrease the burden and enhance the performance of the AC system by removing LHL from processed air. In the LDDS, the selection of the liquid desiccant is very crucial for the regeneration and dehumidification process [13]. An appropriate liquid desiccant for an LDDS should possess a number of characteristics, such as availability, non-corrosive, low regeneration temperature, low viscosity, low equilibrium vapor pressure, high heat transfer, low surface tension, non-volatile, stability, and low cost [14]. CaCl_2 , lithium bromide (LiBr), LiCl , and magnesium chloride (MgCl_2) are the most frequently employed liquid desiccants in LDDS, and their dehumidification and regeneration capabilities are widely utilized in recent engineering applications [15]. LiCl , the most stable liquid desiccant, has the lowest dehydration concentration (30–40%) and the lowest vapor pressure [16]. LiBr is approximately 20% more

costly than LiCl, but it possesses the same regeneration and dehumidification capabilities. As the most readily available desiccant, CaCl₂ solution has the lowest cost but can be unstable depending on the solution's concentration and the air conditions at the inlet [17]. Moreover, the dehumidifier in the LDDS system was equipped with an external cold source for internal cooling, consequently lowering the solution temperature and enhancing overall dehumidification capacity. During experiments and technical applications, however, it was noticed that saline liquid desiccant caused severe erosion on metal dehumidifiers, which are typically constructed from metal. Therefore, researchers explore more alternatives for new liquid desiccant solutions.

Among all liquid desiccant materials [18], potassium formate (KCOOH) has gained popularity among researchers as it has a non-corrosive nature, is environmentally friendly, non-toxic, low manufacturing cost, and low viscosity compared to commonly used liquid desiccants. Moreover, the KCOOH has a high vapor pressure, thus it requires less energy consumption during the regeneration process [19]. Longo et al. [20] studied the performance of desorption and regeneration of KCOOH and LiBr liquid desiccants and experimental results concluded that the LiBr performed well compared to KCOOH solution in terms of dehumidification performance. Nevertheless, the regeneration performance was found to be better than that of LiBr. In another study [21], they performed an experimental and simulation on the performance of KCOOH solution, and the results showed that the weak or diluted liquid desiccant can be regenerated at a temperature of around 40–50 °C, which is achieved using renewable energy sources. Longo et al. [22] measured thermal conductivity and dynamic viscosity of KCOOH solution having a concentration between 60 and 80% and a temperature range of 1–80 °C. The result revealed that the thermal conductivity of KCOOH was 23–33% lower than water at a similar temperature, and the sensitivity of relative viscosity towards salt concentration was strong and weak or low towards temperature for a concentration range of 70%. Moreover, dynamic viscosity for higher a concentration range (above 75%) shows greater sensitivity, i.e., 4–30 times greater sensitivity compared to water. Wen et al. [23] examined the thermal properties and mass transfer performance of KCOOH solution, and results revealed that inlet air temperature and inlet solution flow rate have less influence on the performance of mass transfer, whereas air humidity and solution temperature greatly affect the absolute moisture change. Moreover, a film shrinkage model was developed which shows the accuracy in predicting the falling film (actual) with a deviation of 3.4%. In another study [24], the authors experimentally investigated the regeneration performance of KCOOH solution and the corrosion behavior of 316 L stainless steel with KCOOH and LiCl solution. They also presented vapor pressure data for the KCOOH solution and found that at a certain temperature range of desiccant solution (45–65 °C), the vapor pressure of KCOOH solution having a concentration range of 64.3–73.3% has the same value as that of LiCl solution having a concentration range of 33–38%. In addition, by employing KCOOH solution in place of LiCl solution, the price of liquid desiccant may be reduced from 1081 to 1.50 USD/kg, a substantial savings. Zhang et al. [25] developed a novel heat recovery system consisting of an LDDS and a VCS unit with a return water temperature of 60 °C. In this proposed system, R134a was selected as the refrigerant and KCOOH as the liquid desiccant. The parametric analysis recommended that the gas flow rate range should be between 3.2 and 3.4 with a liquid desiccant temperature of 45 °C. Under these conditions, the efficiency (thermal) was enhanced from 90 to 104%, with a savings of USD 34,000 per month. Hong et al. [26] experimentally researched KCOOH by employing electro dialysis and the effects of operating conditions on the parameters were analyzed. The results revealed that with an increase in desiccant concentration, the area-specific resistance will increase. However, there will be a decrease in overall transport numbers and hydration numbers. Furthermore, when the temperature of the solution is reduced from 21 to 30 °C, the ASR decreases from 21 to 17% at different concentrations. Cheng et al. [27] designed a novel cascade AC system with working pair of LiBr and KCOOH solution and powered by low-grade energy below 80 °C for effective and deep waste heat utilization, which includes an absorption

chiller and an LDDS. The result is a decrease in indoor temperature from 34.5 to 22 °C. The system's cooling capacity was found to be 11.5 kW when working with LiBr and 10.2 kW while working with KCOOH. Furthermore, the COP of the system is the same for both solutions when the solution flow rate is low. If the solution flow rate is high, the COP of the LiBr solution is better. Chen et al. [28] conducted an investigation into dehumidification performance of KCOOH solution on a system equipped with a noble hollow fiber. The inlet air velocity (0.65–4.5 m/s), relative humidity (55–75%), and desiccant concentration (62%, 49%, and 36%) were selected as input variables. The result indicates that the advance in air velocity causes a decrease in sensible and latent effectiveness but an increase in moisture removal rate (MRR). Moreover, as desiccant concentration increased, the MRR also increased with a decrease in latent effectiveness.

The literature confirms that hybridization of LDDS with VCS can be a highly efficient energy-saving technique in tropical climates where waste heat or renewable energy can be utilized to increase the efficiency of the system. Despite significant contributions made by previous researchers, there are still unexplored research areas. It is also found that the researchers put little emphasis on the research of KCOOH (experimentally and numerically) compared to other more often employed saline solutions. The study related to the dehumidification performance of KCOOH solution in such small-scale HLDAC systems is rare and has not yet been explored in existing studies. As far as the authors are concerned, the design of experiments (DOE) approach has not yet been used to optimize the process parameters of dehumidification performance of KCOOH liquid desiccant in the HLDAC system. In this study, we propose a novel HLDAC system combined with a VCS unit with KCOOH as the working liquid desiccant. Furthermore, the experimental runs are designed according to response surface methodology (RSM) to develop the experiments correlations for dehumidification performance of various influencing parameters. Furthermore, a comparative evaluation of the dehumidification performance between the HLDAC system and conventional VCS was conducted. This paper also contains an investigation of the load sharing between the dehumidifier of HLDAC and the evaporator of the VCS unit operating under hot and humid conditions. A fair economic comparison and a payback period calculation are performed to figure out how much more energy the HLDAC system saves than the standalone VCS unit.

2. Description of Experimental Setup

As in [29], the proposed small-scale HLDAC system consists of a fabricated non-corrosive KCOOH liquid desiccant dehumidification/regeneration system and an R134a refrigerant-driven 1 TR capacity VCR unit as demonstrated in Figure 1. The major sections are the dehumidifier section, regenerator section, solution-water heat exchanger (SW-HX), air-air heat exchanger (AA-HX), a sealed compressor, fin-tube type evaporator, capillary tube for expansion, air-cooled condenser, centrifugal pump, centrifugal blower, solution tank, and collection tank. While designing and fabricating the experimental test rig, all possible problems and requirements are taken into consideration. The authors' [30] design guidelines were utilized for calculating the size of the structured packing chamber. The dehumidifier section and regenerator section are the core of the LDDS system. They transfer heat and moisture between air and liquid desiccant solution and are functionally identical. First, the capacity of the dehumidifier section is determined as 2.5 kW. Based on the amount of air and solution flow rates, the cross-sectional area of the dehumidifier and its structured packing are selected. With the help of heat and mass transfer correlation, the height of the dehumidifier section is computed to be 1 m under the assumption that the moisture content and thermal efficiency are 0.65. The packed-bed type counter-flow dehumidifier section with adiabatic cooling is made up of transparent acrylic material with polyvinyl chloride (PVC) sheets as packing material. The overall length, width, and height of the dehumidifier section are 1 m, 0.4 m, and 0.4 m, respectively, while the packaging material is 0.4 m, 0.4 m, and 0.4 m respectively. The height of the packing material is adjustable while

its cross section is the same as that of the dehumidifier section. The dimensions of various components of LDDS are given in Table 1.

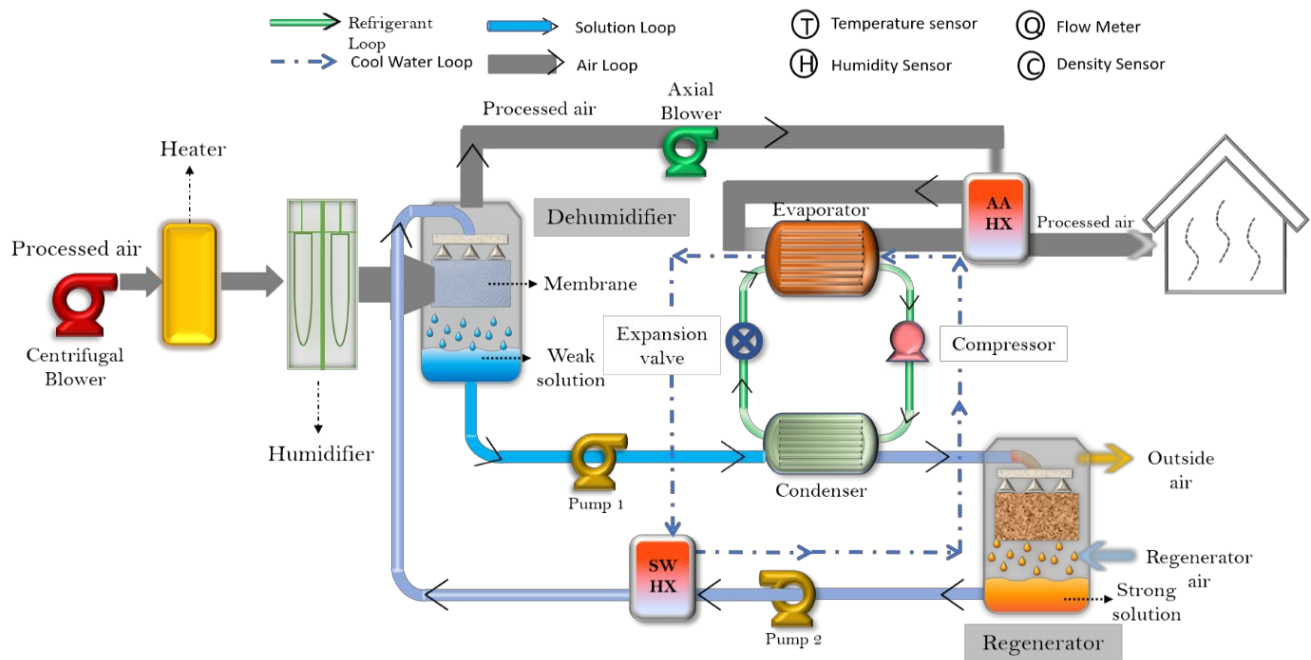


Figure 1. The schematic diagram of proposed HLDAC system.

Table 1. The devices employed in the test rig and dimensions of HLDAC.

Items	Dimensions/Capacity
Packing length	0.4 m
Packing width	0.4 m
Packing height	0.6 m
Liquid desiccant	Potassium formate
Centrifugal blower capacity	140 W (1 quantity)
Anti-corrosive pump capacity	0.75 kW
Sealed compressor capacity	3.5 kW (1 quantity)
Axial blower capacity	140 W (1 quantity)
Electric heater capacity	500 W (2 quantity)

In this research, KCOOH is employed as a liquid desiccant solution for economic, environmental, and non-corrosive reasons. The incoming fresh strong (concentrated) KCOOH solution from the storage tank is pumped and sprayed across the dehumidifier packed tower with the help of an anti-corrosive solution pump and spray nozzles made up of PVC pipe of 0.5 inches. The flow rate of the liquid desiccant is regulated by the control valves. The KCOOH solution is prepared with the help of distilled water. For the experimental trials, the artificial hot and humid inlet air at the dehumidifier inlet is maintained by an electric heater and a steamer that are available in the laboratory. With the help of an axial blower that is employed after the dehumidifier exits, the air will regain its flow rate that was decreased because of a drop in pressure in the dehumidifier section. The dehumidified air subsequently enters the AA-HX for heat recovery by releasing heat into the evaporator's cold stream. This precooled air is then directed to the evaporator of the VCS unit, where the remaining heat load is managed. The difference in vapor pressure is the main cause of driving force to absorb the moisture content from the ambient humid

air. After absorbing moisture, it becomes weak or diluted, and then it is transferred to a weak storage tank through an exit hole provided at a certain level at the bottom of the dehumidifier. However, to increase the efficiency or effectiveness of the proposed HLDAC system, the waste heat from the condenser is utilized to regenerate weak solution. This weak desiccant is heated by the condenser coils and then transferred to the regenerator for the regeneration process. In a regenerator, weak desiccant solution is regenerated to its original state as the moisture from it is transferred to the ambient air, which has a lower vapor pressure than the weak solution. In this way, the weak desiccant is regenerated, but its temperature is high. It is passed to the SW-HX to lower the temperature of a strong desiccant solution. In SW-HX, cool water is employed whose temperature is lowered by passing it through the evaporator coils of the VCR unit. This is how the performance of the HLDAC system was increased by employing the waste energy in the experimental test rig. In a case where waste heat from the condenser outlet does not satisfy the criteria, an external electric heater of 500 W is employed in the path to heat the ambient air for regeneration purposes. Two blowers, one centrifugal and one axial, are used to keep the air flow going in a certain direction. During experiment trials, all the parameters that are required to analyze the dehumidification performance are measured by employing respective sensors or devices at different locations in the experimental setup. The desiccant solution concentration is determined by measuring the specific gravity of the solution with a hydrometer. The flow rate of the solution is determined by choosing a vessel with a given volume and monitoring the time required for filling the vessel using a stop watch. By placing a digital anemometer, the air flow rate is monitored. The energy consumed data are measured by an energy meter attached to the control panel. The specifications of all the devices employed in this experimental setup are given in Table 2.

Table 2. Measuring instruments with their specifications and uncertainties.

Device	Type	Accuracy	Range
Thermometer	PT100 RTD	± 0.1 °C	(−50)–200 °C
Densitometer	Specific gravity hydrometer	± 1 kg/m ³	1000–1400 kg m ^{−3}
Humidity transducer	HF535-W, HC2-S3	$\pm 1\%$ RH	0–100% RH
Anemometer	CP218-BO differential pressure flowmeter	$\pm 2\%$ m s ^{−1}	0–30 m s ^{−1}
Solution temperature	T-type thermocouple	± 0.2 °C	0–200 °C

The consistency of the measured parameters (dependent or independent) can be estimated by uncertainty analysis [31]. In this study, the uncertainty of the dependent and independent variables is given in Table 3. It can be noted that all variables have uncertainty errors within $\pm 6\%$ which is acceptable in engineering applications [32]. The equations related to heat and mass transfer across the dehumidifier or regenerator section are obtained by applying the principle of mass and energy conservation developed by the authors [33]. Let us consider a small differential element of length dZ as shown in Figure 2. While designing and developing components of the experimental setup, the following assumptions were considered [34]:

- The dehumidifier and regenerator are adiabatic with no desiccant carryover.
- The distribution of desiccant solution and air is considered uniform throughout the whole section.
- The interfacial area (area of contact) between air and desiccant is the same.
- The pressure-drop across connecting pipes is considered negligible.
- The exit states of an evaporator and condenser are considered saturated.
- Expansion valve heat loss is negligible.
- Heat transfer resistance is considered more negligible for the liquid phase than that of the gaseous phase.

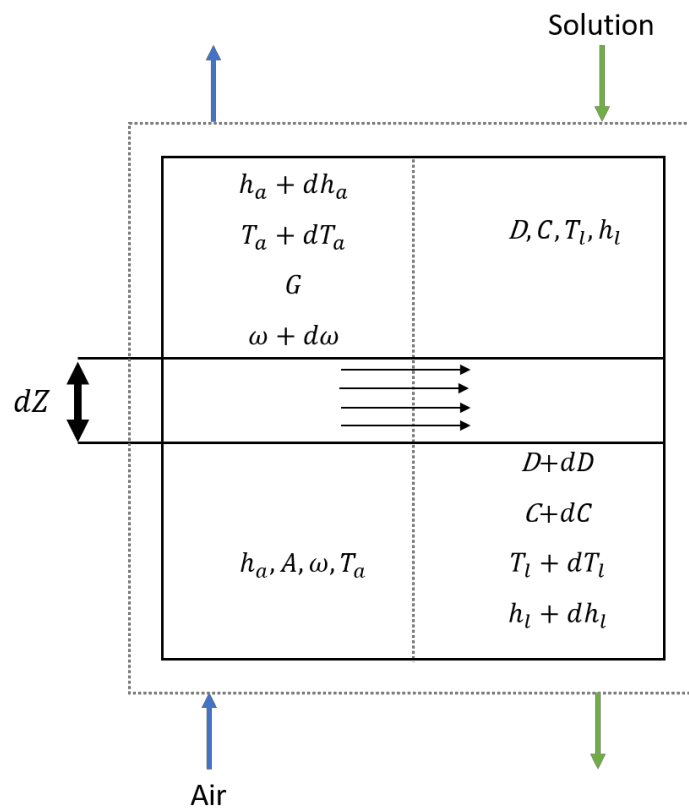


Figure 2. Schematic of differential element for heat and mass transfer process.

The mass balance equation across this element is given by [34]:

$$D + dD + A\omega = D + A(\omega + d\omega) \quad (1)$$

The above equation can be simplified to the change in desiccant flow as a function of change in air humidity ratio, and can be expressed as follows [34]:

$$\frac{dD}{dZ} = A \frac{d\omega}{dZ} \quad (2)$$

Moreover, Equation (3) depicts a mass balance equation for water vapor over this small element [34]:

$$N_v M_v a_t dZ + A(\omega + d\omega) = A\omega \quad (3)$$

where, N_v can be defined as [34]:

$$N_v = F_G \ln \left[\frac{1 - y_i}{1 - y} \right] \quad (4)$$

Equation (3) yields the change in air humidity ratio across differential element [34]:

$$\frac{d\omega}{dZ} = \frac{-M_v F_G a_t}{A} \ln \left[\frac{1 - y_i}{1 - y} \right] \quad (5)$$

The mass balance for water is given by [34]:

$$[(1 - C) + d(1 - C)](L + dL) + A\omega = A(\omega + d\omega) + L(1 - C) \quad (6)$$

The energy balance equation differential element is given by [34]:

$$q_G a_t dZ + N_v M_v a_t h_v dZ + A(h_a + dh_a) = Ah_a \quad (7)$$

Because $h_a = h_a(T_a, \omega)$, the change in h_a can be determined from partial derivatives of h_a [33]:

$$dh_a = \frac{\partial h_a}{\partial T_a} dT_a + \frac{\partial h_a}{\partial Y} d\omega \quad (8)$$

Therefore, we obtain [35]:

$$dh_a = (c_{pa} + \omega c_{pV}) dT_a + (c_{pV}(T_a - T_0) + \lambda_0) d\omega \quad (9)$$

The final balance (thermal) equation is given by [35]:

$$Ah_a + (D + dD)(h_L + dh_L) = A(h_a + dh_a) + Dh_L \quad (10)$$

Simplifying Equation (10) and neglecting $dDdh_L$ gives [35]:

$$Ddh_l + h_l dD = Adh_a \quad (11)$$

Neglecting the heat of mixing, the enthalpy of the desiccant is given by [34]:

$$h_l = c_{pl}(T_l - T_0) \quad (12)$$

Thus [34],

$$dh_l = c_{pl} dT_l \quad (13)$$

By putting combining Equations (2), (9), and (11)–(13), you can find the expression for the change in temperature of the desiccant solution across the given element [16]:

$$\frac{dT_l}{dZ} = \frac{A}{Dc_{pl}} \left\{ (c_{pa} + \omega c_{pV}) \frac{dT_a}{dZ} + [c_{pV}(T_L - T_0) - c_{pL}(T_L - T_0) + \lambda_0] \frac{d\omega}{dZ} \right\} \quad (14)$$

The effectiveness of the dehumidifier is defined as the amount of actual moisture absorbed to the maximum possible, and can be expressed as [16]:

$$\epsilon = \frac{\omega_1 - \omega_2}{\omega_1 - \omega_i} \quad (15)$$

where ω_1 and ω_2 are the air humidity ratios of the dehumidifier, respectively, while ω_i is the equilibrium air humidity ratio.

Table 3. Experimental uncertainty of the calculated parameters.

Parameters	Uncertainty	Range
Air temperature	± 0.2 °C	15–40 °C
Air relative humidity	$\pm 1\%$	45–75%
Inlet desiccant temperature	± 0.3 °C	28–35 °C
Air flow rate	$\pm 3.56\%$	
Air velocity	± 0.1	2–10
COP of a hybrid system	$\pm 5.45\%$	
Heat load of dehumidifier	$\pm 5.32\%$	

3. DOE Methodology

DOE is a powerful statistical tool to analyze the behaviors of input and output variables and to optimize the response parameters for different combinations of experimental trials. By employing the DOE technique, the amount of time and cost of experimentation can be reduced by analyzing various independent variables and a substantial interaction between

the variables [36]. Among numerous design models, RSM is the most effective methodology that incorporates a popular design [37].

RSM is a group of statistical tools that can be used to establish a mathematical connection between a monitored response and the input parameters aiming at process optimization. There are two important factors which are commonly used in RSM [38]. A first-order model for an independent variable (k) can be depicted as [37]:

$$y = \beta_0 + \sum_{i=1}^k \beta_i x_i + \varepsilon \quad (16)$$

The second-order (quadratic) model employed is given by:

$$y = \beta_0 + \sum_{i=1}^k \beta_i x_i + \sum_{<j=2}^k \sum_{<j=2}^k \beta_{ij} x_i x_j + \sum_{j=1}^k \beta_{jj} x_j^2 + \varepsilon \quad (17)$$

where ε represents the random experimental error, which results from the unexpected behaviour in y , and is usually assumed to be normally distributed with constant variance. The y is the response of interest which is a function of factors $x = (x_1, x_2, \dots, x_k)$. β represents the vector of unknown constant coefficient referred to as parameters.

The first-order designs are depicted by 2^k factorial while second order designs are given 3^k factorial designs, Box–Behnken design, central composite design (CCD), etc. The CCD is the most often employed fractional factorial design in RSM [38]. It is an integral part of RSM that is most appropriate or widely accepted for second-order design techniques for optimizing the research problems. It is a combination of two-level factorial or fractional factorial design points (2^k) and $2k$ axial points (also called star points) as well as centre points (n). The centre points give a good and independent estimate of experimental errors. The total number of experiments are given by:

$$N = 2^k + 2k + n \quad (18)$$

where k represents the number of variables studied, and n is the number of replicas.

As illustrated in Figure 3, the RSM methodology for optimization might be categorized into six phases: (a) selecting input variables and responses parameters; (b) selecting experimental design methodology; (c) performing experimental runs; (d) fitting model equation to experimental data; (e) obtaining response graphs and model validation; and (f) assessment of optimal conditions.

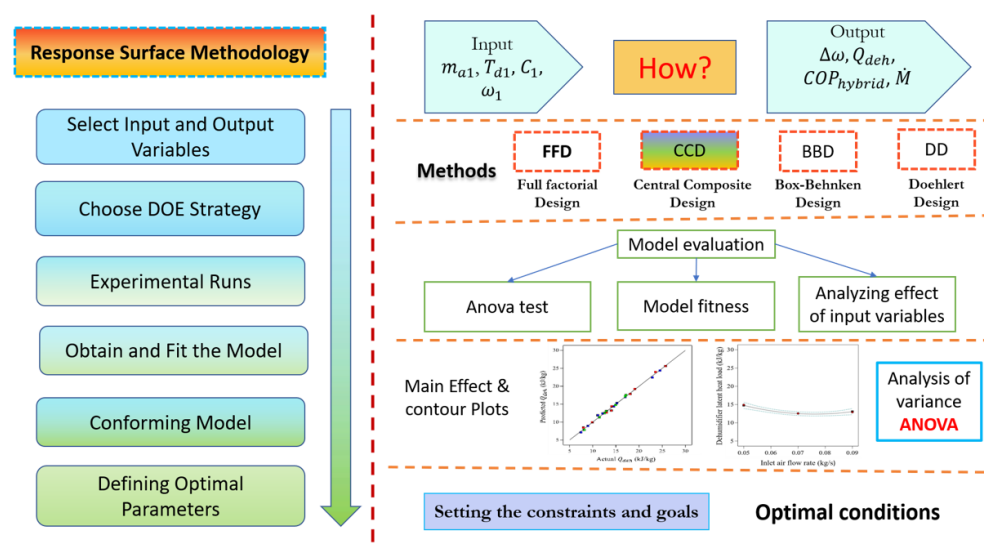


Figure 3. Flow chart of RSM methodology.

3.1. Experimental Design

In this study, CCD was used to determine the optimum conditions of performance of dehumidification of KCOOH solution. The investigation of the performance of the HLDAC system was performed by employing RSM and CCD techniques. Four independent variables (factors) were chosen as A: inlet air flow rate; B: inlet desiccant temperature; C: inlet desiccant concentration, and D: inlet specific air humidity. Table 4 summarizes the four input variables and their levels.

Table 4. Independent variables and their corresponding levels.

Independent Variables	Symbol	Units	Coded Levels ^a		
			−1	0	+1
Inlet air flow rate	m_{a1}	kg/s	0.05	0.07	0.09
Inlet desiccant temperature	T_{d1}	°C	29	32	35
Inlet desiccant concentration	C_1	kg _{des} /kg _{sol}	0.65	0.68	0.71
Inlet specific air humidity	ω_1	g/kg	15	20	25

^a−1: low level, 0: middle level, +1: high level.

The different values of these input variables are chosen based on the viability of the environmental circumstances. To prevent desiccant carryover of the desiccant solution, the air flow rate is kept low [39]. The temperature range of desiccants is determined by environment conditions [39]. Moreover, the different values of the concentration of desiccant are selected in order that they can provide the driving force for moisture removal [40]. The flow rate of desiccant solution is kept constant at 0.08 kg/s for the reason that its influence is subordinate to the air flow rate [41]. During all experiment trials, the inlet air temperature was maintained at a constant value of 36 °C because it is beneficial to do so. This constant temperature is maintained by the assembly attached to this experimental setup. The assembly consists of a heater and a steamer in which the heater is utilized to maintain a constant air temperature while the steamer is utilized to change the humidity level of the air according to the requirements of the experimental trial. These devices are connected to on-off based on the signal provided by the sensors. The design of expert software was utilized to design the experimental trials with four factors and three levels. A total of 25 experiments were designed by applying the RSM-CCD technique.

3.2. Performance Indicators

The whole experiment is conducted to evaluate the dehumidification performance of KCOOH solution; the following three responses were selected and analyzed based on the criteria of the developed HLDAC system, and are suggested here.

3.2.1. Dehumidifier Latent Heat Load (Q_{deh})

The amount of latent heat load managed by the dehumidifier unit in the respective proposed HLDAC system is determined by the following expression:

$$Q_{deh} = c_{pa} \times (T_{a1} - T_{a2}) + \Delta h_{abs} \times (w_{a1} - w_{a2}) \quad (19)$$

where Δh_{abs} can be expressed as follows:

$$\Delta h_{abs} = h_{fg}(T_a, w) + \Delta h_{dil}(T_d, C) \quad (20)$$

3.2.2. Coefficient of Performance of the HLDAC System (COP_{hybrid})

The coefficient of performance of the HLDAC system can be expressed as follows:

$$COP_{hybrid} = \frac{\dot{Q}_{deh} + \dot{Q}_{VCR}}{\dot{Q}_{reg} + \sum W} \quad (21)$$

where \dot{Q}_{deh} and \dot{Q}_{VCR} are the dehumidifier latent heat removal rate and the heat removed by the VCS unit, respectively. In addition, Q_{reg} represents the amount of heat required by the regenerator for regeneration of desiccant. ΣW represents the total amount of energy utilized by the HLDAC system, which includes the air heater, solution pump, compressor, condenser, and air blower (two). The following expression can be used to compute \dot{Q}_{VCR} 's value:

$$\dot{Q}_{VCR} = \dot{m}_a \left[c_{pa} \times (T_{a3} - T_{a4}) + h_{fg} \times (w_{a3} - w_{a4}) \right] \quad (22)$$

3.2.3. Moisture Removal Rate (\dot{M}) (g/s)

The moisture removal rate (\dot{M}) is defined as the ability of the dehumidifier to absorb moisture, and it can be calculated from:

$$\dot{M} = \dot{m}_a (\omega_1 - \omega_2) \quad (23)$$

where ω_1 and ω_2 are the dehumidifier's inlet and outlet air humidity ratio.

4. Result and Discussions

4.1. Fitting the Model

The effects of input variables on all three response parameters are given in Table 5. The 25 experimental runs were performed as the experimental design suggested by the RSM-CCD approach under constant inlet air temperature ($T_{a1} = 36$ °C). All three responses are to be maximized.

Table 5. RSM experimental design and the experimental results.

Run	Independent Variables				Responses Values		
	m_{a1} (kg/s)	T_{d1} (°C)	C_1 (kg _{des} /kg _{sol})	ω_1 (g/kg)	Q_{deh} (kJ/kg)	COP_{hybrid} Value	\dot{M} (g/s)
1	0.05	29	0.65	15	14.56	1.85	1.62
2	0.09	29	0.65	15	12.16	1.86	1.76
3	0.05	35	0.65	15	8.96	1.79	1.56
4	0.09	35	0.65	15	7.46	1.75	1.63
5	0.05	29	0.71	15	24.51	2.18	1.98
6	0.09	29	0.71	15	22.89	2.14	2.76
7	0.05	35	0.71	15	17.01	1.98	1.59
8	0.09	35	0.71	15	15.23	1.86	1.67
9	0.05	29	0.65	25	14.09	1.84	1.96
10	0.09	29	0.65	25	12.99	1.85	2.19
11	0.05	35	0.65	25	9.88	1.79	1.59
12	0.09	35	0.65	25	7.98	1.76	1.65
13	0.05	29	0.71	25	25.71	2.21	2.89
14	0.09	29	0.71	25	23.56	2.17	3.01
15	0.05	35	0.71	25	19.09	1.99	1.63
16	0.09	35	0.71	25	18.08	1.87	1.75
17	0.05	32	0.68	20	14.91	1.88	1.91
18	0.09	32	0.68	20	12.92	1.81	2.03
19	0.07	29	0.68	20	16.99	1.93	2.56

Table 5. Cont.

Run	Independent Variables				Responses Values		
	m_{a1} (kg/s)	T_{d1} (°C)	C_1 (kg _{des} /kg _{sol})	ω_1 (g/kg)	Q_{deh} (kJ/kg)	COP_{hybrid} Value	\dot{M} (g/s)
20	0.07	35	0.68	20	11.46	1.8	1.79
21	0.07	32	0.65	20	8.16	1.78	1.92
22	0.07	32	0.71	20	17.19	2.01	2.31
23	0.07	32	0.68	15	11.09	1.81	1.99
24	0.07	32	0.68	25	14.02	1.83	2.29
25	0.07	32	0.68	20	12.56	1.82	2.16

The regression analysis is conducted, and experimental correlation is established. Using experimental data, the coefficients of a polynomial equation were assessed to determine response values. The correlation coefficients for each response variable are reported in Table 6.

Table 6. Regression correlations developed.

Response	Regression Equations
Q_{deh}	$= 167.474 - [613.093 \times m_{a1}] - [10.0162 \times T_{d1}] + [22.0152 \times C_1] - [1.98114 \times \omega_1] + [1.125 \times m_{a1} \times T_{d1}] + [35.4167 \times m_{a1} \times C_1] + [0.7125 \times m_{a1} \times \omega_1] - [5.375 \times T_{d1} \times C_1] + [0.01725 \times T_{d1} \times \omega_1] + [2.08333 \times C_1 \times \omega_1] + [3541.74 \times m_{a1}^2] + [0.191855 \times T_{d1}^2] + [196.328 \times C_1^2] + [0.0022678 \times \omega_1^2]$
COP_{hybrid}	$= 25.024 + [21.1676 \times m_{a1}] + [0.0755675 \times T_{d1}] - [76.3839 \times C_1] - [0.00620304 \times \omega_1] - [0.260417 \times m_{a1} \times T_{d1}] - [28.125 \times m_{a1} \times C_1] + [0.00625 \times m_{a1} \times \omega_1] - [0.479167 \times T_{d1} \times C_1] - [0.000042 \times T_{d1} \times \omega_1] + [0.0375 \times C_1 \times \omega_1] + [35.3107 \times m_{a1}^2] + [0.00379159 \times T_{d1}^2] + [71.2492 \times C_1^2] - [0.000435028 \times \omega_1^2]$
\dot{M}	$= -45.4172 + [0.361111 \times m_{a1}] + [1.47595 \times T_{d1}] + [62.7361 \times C_1] + [0.153958 \times \omega_1] - [0.979167 \times m_{a1} \times T_{d1}] + [62.5 \times m_{a1} \times C_1] - [0.3375 \times m_{a1} \times \omega_1] - [2.01389 \times T_{d1} \times C_1] - [0.00733333 \times T_{d1} \times \omega_1] + [0.191667 \times C_1 \times \omega_1]$

The experimental data can be represented by a quadratic polynomial model, according to the analysis of variance (ANOVA) results. Table 7 displays the coefficient of determination (R^2) value. Moreover, the model robustness is visualized in Figure 4.

Table 7. Regression coefficients for output responses.

Regression Coefficients	Q_{deh}		COP_{hybrid}		\dot{M}	
		SSV		SSV		SSV
Intercept	12.51	644.7 (model)	1.83	0.4621 (model)	1.98	3.98 (model)
A—Inlet air flow rate	−0.8583 ***	13.26	−0.0244 ***	0.0108	0.0956 **	0.1644
B—Inlet desiccant temperature	−2.91 ***	152.02	−0.0800 ***	0.1152	−0.3261 ***	1.91
C—Inlet desiccant concentration	4.84 ***	420.79	0.1189 ***	0.2544	0.1950 ***	0.6845
D—Inlet air humidity	0.6406 ***	7.39	0.0050	0.0005	0.1300 ***	0.3042

Table 7. Cont.

Regression Coefficients	Q_{deh}		COP_{hybrid}		\dot{M}	
		SSV		SSV		SSV
A^2	1.42 ***	5.11	0.0141	0.0005	−0.0841	0.018
B^2	1.73 ***	7.59	0.0341 ***	0.003	0.1209	0.0372
C^2	0.1767	0.0795	0.0641 ***	0.0105	−0.0391	0.0039
D^2	0.0567	0.0082	−0.0109	0.0003	−0.0841	0.018
AB	0.0675	0.0729	−0.0156 ***	0.0039	−0.0588	0.0552
AC	0.0212	0.0072	−0.0169 ***	0.0046	0.0375	0.0225
AD	0.0712	0.0812	0.0006	0.0000625	−0.0338	0.0182
BC	−0.4838 **	3.74	−0.0431 ***	0.0298	−0.1813 ***	0.5256
BD	0.2587 **	1.07	−0.0006	0.0000625	−0.1100 **	0.1936
CD	0.3125 *	1.56	0.0056	0.0005	0.0287	0.0132
R^2	0.9958		0.9966		0.9627	

*** denotes p -value < 0.001, ** denotes p -value < 0.01, and * denotes p -value < 0.05.

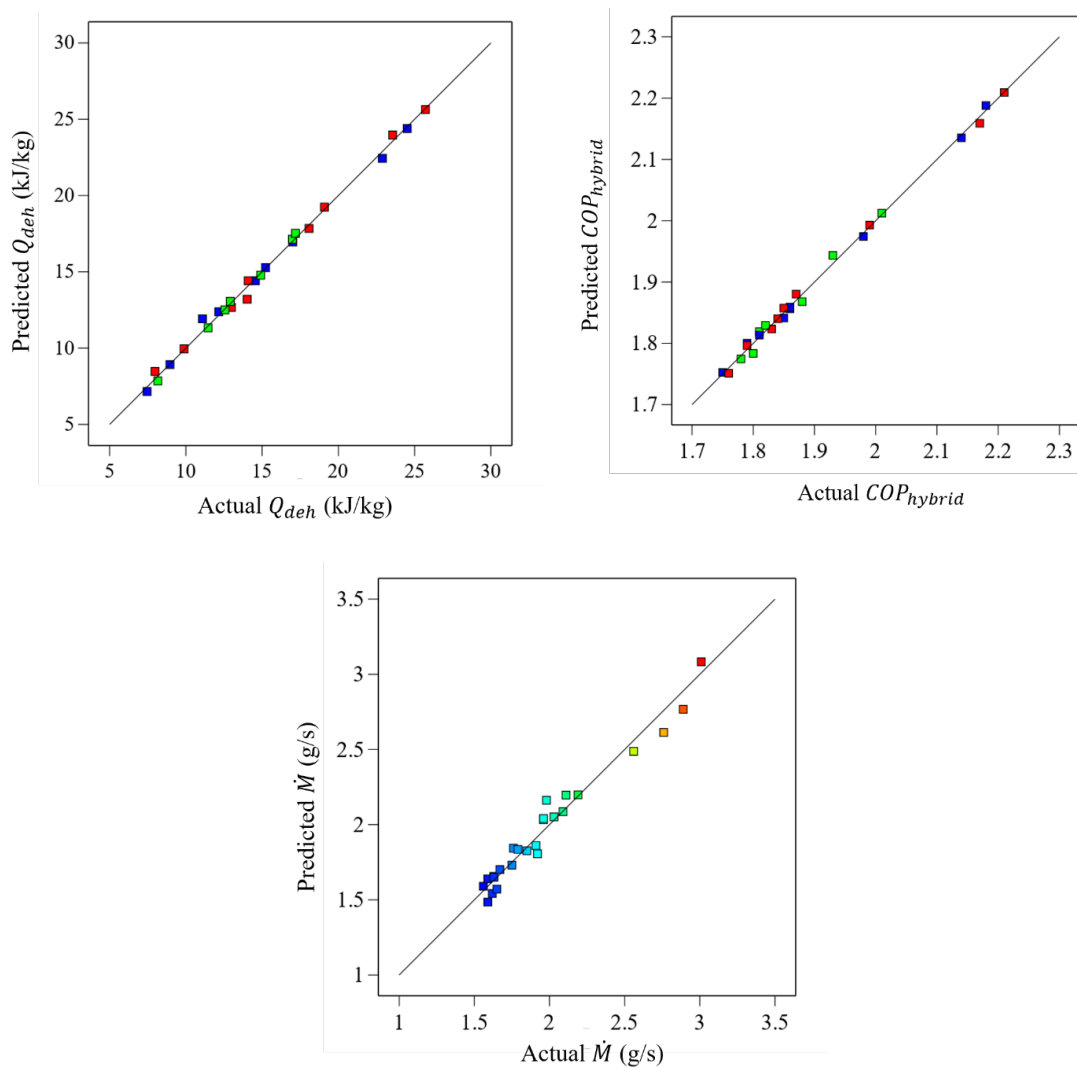


Figure 4. Actual vs. predicted values plots for responses.

4.2. Effect of Input Variables on Response Parameters

From Table 5, it can be observed that there is a major change in all responses for each combination of experimental runs. From the results, it can be observed that with an increase in inlet air flow rate, desiccant concentration, and specific air humidity, all three responses (Q_{deh} , COP_{hybrid} , and \dot{M}) will increase. Moreover, the same effect of the inlet desiccant temperature is observed on Q_{deh} and COP_{hybrid} , whereas by increasing the inlet desiccant temperature, the \dot{M} is reduced. Furthermore, from experimental run 13, it can be observed that the maximum values of Q_{deh} and COP_{hybrid} are obtained with a minimum level of m_{a1} , T_{d1} and a maximum level of C_1 , ω_1 . On the other hand, the minimum values of Q_{deh} and COP_{hybrid} are obtained with a maximum level of m_{a1} and T_{d1} and a minimum level of C_1 and ω_1 (i.e., run 4). For the 3rd and last response, i.e., \dot{M} , the maximum value is obtained with the maximum level of m_{a1} , C_1 , and ω_1 and a minimum level of T_{d1} (run 14). On the other hand, the minimum value of \dot{M} is obtained with the minimum levels of m_{a1} , C_1 , and ω_1 and the maximum level of T_{d1} (run 3). Therefore, from the selected above-mentioned experiment runs, the following input variable levels can be selected to obtain optimal output responses.

4.2.1. Dehumidifier Latent Heat Load

Figure 5 illustrates the effect of independent variables on the Q_{deh} response. From the results, the maximum value of Q_{deh} is observed at the lowest values of m_{a1} and T_{d1} . However, the highest values of C_1 and ω_1 yield the maximum value of Q_{deh} . The reason behind the higher heat removal rate at lower air flow rate is due to the fact that the contact or interaction time increases between inlet air and liquid desiccant, which leads to significant MRR compared to high inlet air flow rates. Similarly, at a low inlet desiccant solution temperature, the capacity to absorb moisture content by the solution will be high due to the higher driving force. At an optimal level of mass concentration of desiccant solution, it will be more likely to execute its intended function. Moreover, with the increasing humidity level of inlet air, the value of the dehumidifier's latent heat load will increase. The effect of input variables on the Q_{deh} response can be seen as a quadratic (p -value < 0.001) term with all four input variables. Similar behavior of the input variable is found in the literature [26,42,43]. Furthermore, from the sum-of-squares values as shown in Table 7, a noteworthy significance level of Q_{deh} response is shown. The highest contribution among linear terms of the input variables is that of C_1 , with a 65.27% contribution. The square interaction term T_{d1}^2 has the highest contribution, with 1.17% contribution. The cross-interaction term $T_{d1} \times C_1$ has only 0.58% contribution.

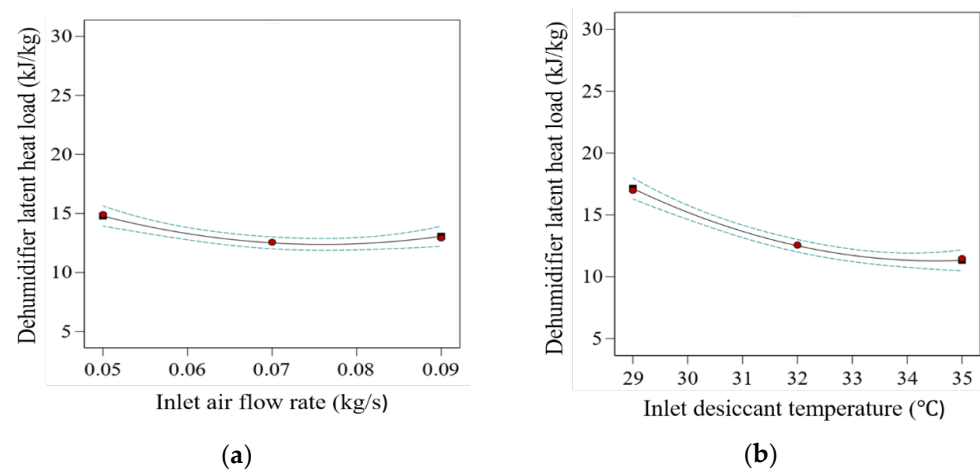


Figure 5. Cont.

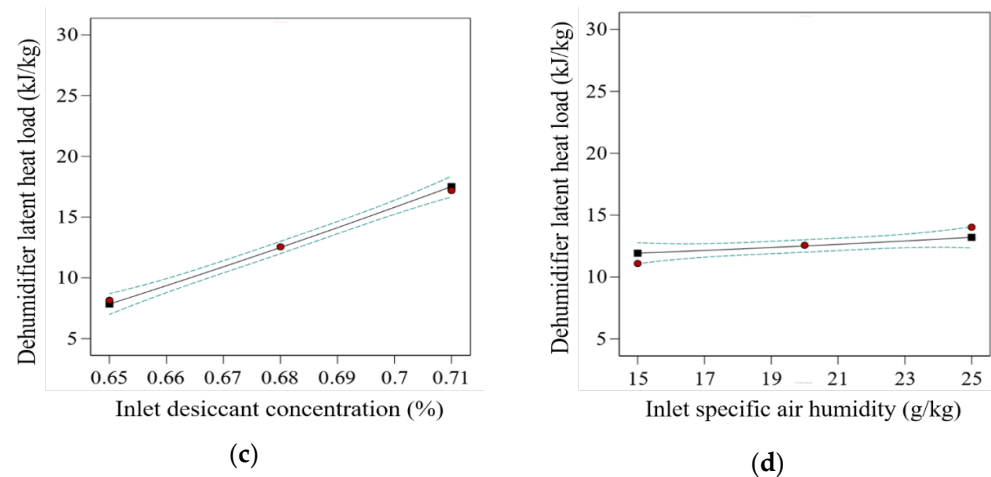


Figure 5. Main effect plots for Q_{deh} versus (a) m_{a1} , (b) T_{d1} , (c) C_1 , and (d) ω_1 .

4.2.2. Coefficient of Performance of the HLDAC System

Figure 6 illustrates the effect of independent variables on the COP_{hybrid} response. From the Figure 6, the C_1 has significant influence as compared to the other three variables as the value of COP_{hybrid} increases from 1.76 to 2.11. Furthermore, the maximum value of COP_{hybrid} is observed at lowest values of m_{a1} and T_{d1} . However, the highest values of C_1 and ω_1 yield the maximum value of COP_{hybrid} . Furthermore, the effect of input variables on the COP_{hybrid} response can be seen in the quadratic (p -value < 0.001) term with three input variables, except for inlet air humidity. Moreover, from the sum of squares values as shown in Table 7, a noteworthy significance level of COP_{hybrid} response is shown. The highest contribution among linear terms of the input variables is that of C_1 , with a 55.05% contribution. The square interaction term C_1^2 has the highest contribution, i.e., 2.27% contribution. The cross-interaction term $T_{d1} \times C_1$ has 6.44% contribution.

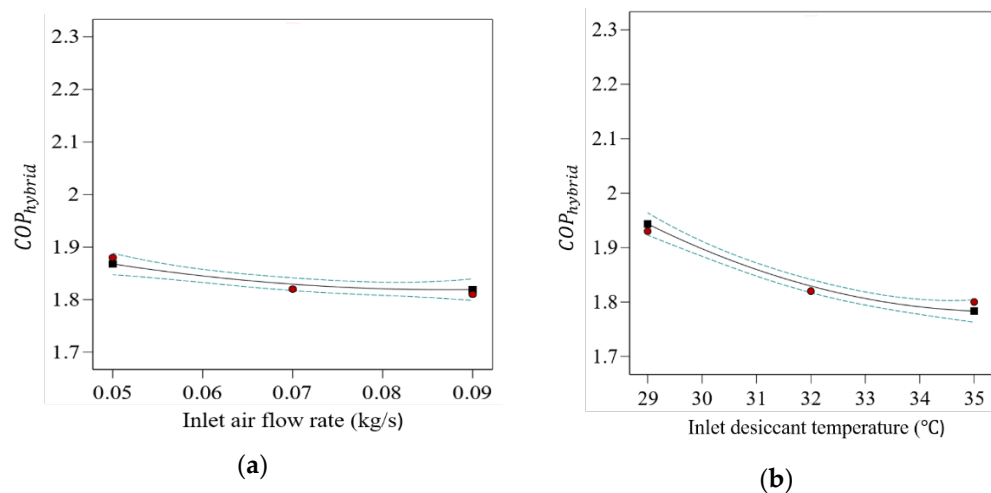


Figure 6. Cont.

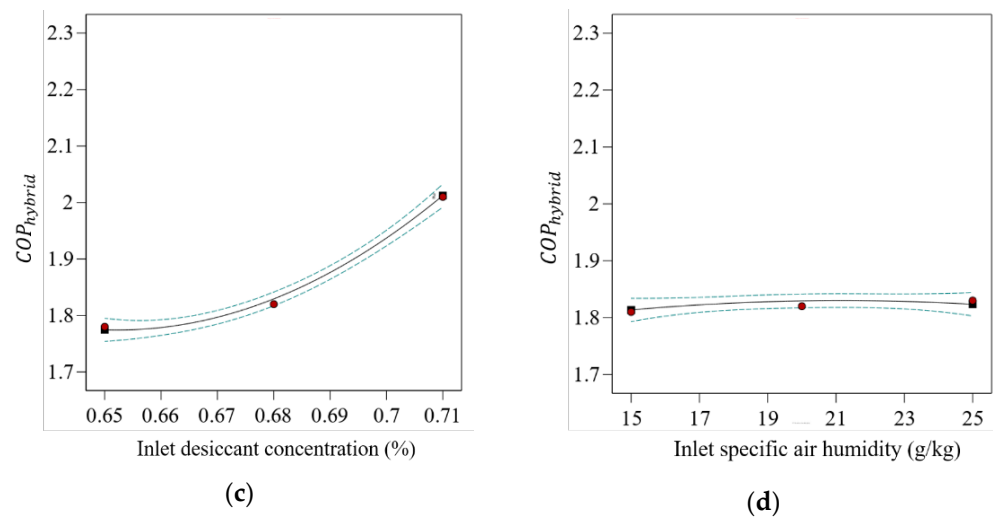


Figure 6. Main effect plots for COP_{hybrid} versus (a) m_{a1} , (b) T_{d1} , (c) C_1 , and (d) ω_1 .

4.2.3. Moisture Removal Rate

Figure 7 illustrates the main effect plot for the 3rd and last response, i.e., \dot{M} . The MRR greatly depends on deviation in vapor pressure between the air and desiccant solution. The higher value of MRR is obtained when inlet air humidity is relatively high. This is because the higher humidity levels in the inlet air represent a higher vapor pressure in it, which leads to a larger vapor pressure difference between the desiccant solution and air. Due to the abovementioned phenomenon, the moisture transfer rate will be higher due to the high vapor pressure difference, which results in a better dehumidification system. From the results, it can be observed that the maximum value of \dot{M} is observed at the highest value of m_{a1} , C_1 , and ω_1 and the lowest value of T_{d1} . Furthermore, from the sum of squares values as shown in Table 7, a noteworthy significance level of \dot{M} response is shown. The highest contribution among linear terms of the input variables is that of T_{d1} , with a 47.98% contribution. The square interaction term T_{d1}^2 has the highest contribution, with 0.93% contribution. The cross-interaction term $T_{d1} \times C_1$ has 13.2% contribution.

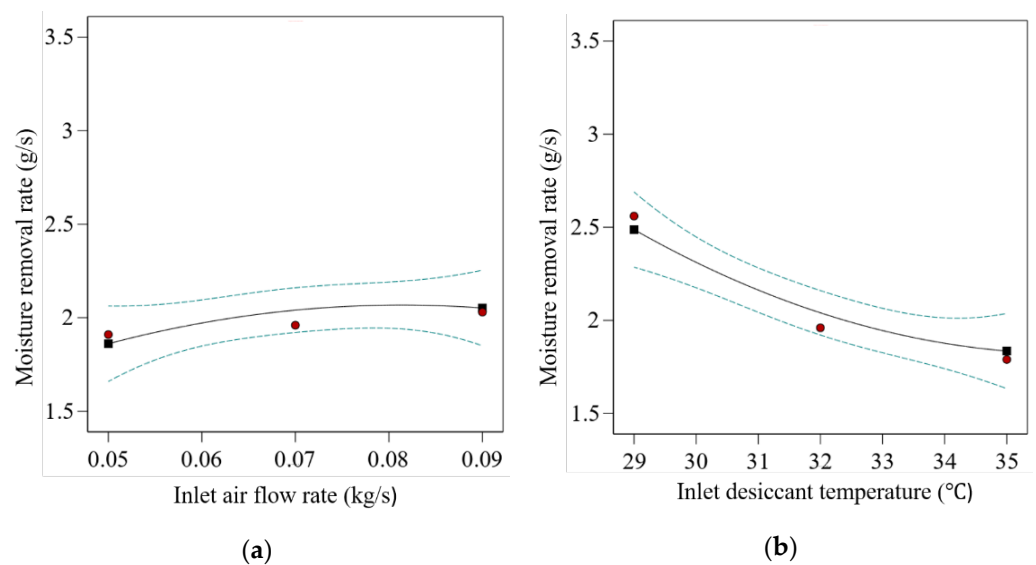


Figure 7. Cont.

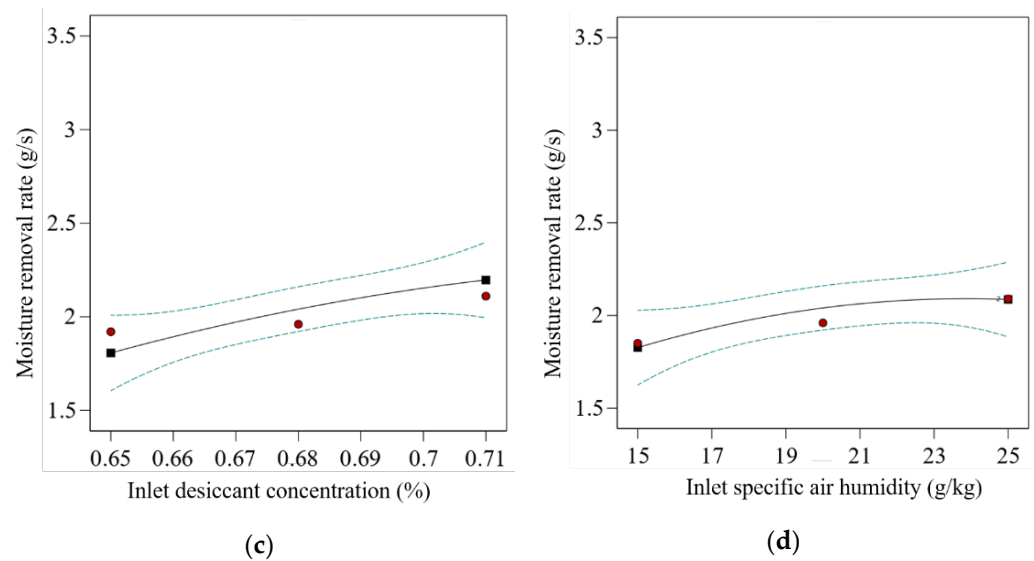


Figure 7. Main effect plots for \dot{M} versus (a) m_{a1} , (b) T_{d1} , (c) C_1 , and (d) ω_1 .

4.3. Optimization and Validation of Model

To analyze the effect of independent input variables, i.e., m_{a1} , T_{d1} , C_1 , and ω_1 , the main effect plots were drawn by employing the design of expert software. Afterwards, the numerical optimization was conducted. The goals selected for the optimization of dehumidification performance of KCOOH solution were minimum levels of m_{a1} and T_{d1} and maximum levels of C_1 and ω_1 in order to obtain maximum Q_{deh} , COP_{hybrid} , and \dot{M} . The combined optimized levels for optimum responses were 0.05 (m_{a1}), 29 (T_{d1}), 0.71 (C_1), and 25 (ω_1). The responses values at optimized conditions were 25.636 (Q_{deh}), 2.209 (COP_{hybrid}), and 2.791 (\dot{M}) as shown in Table 8.

Table 8. Optimum variable levels, experimental and predicted values of response parameters.

Optimum Condition	Coded Levels	Actual Levels
m_{a1}	−1	0.05
T_{d1}	−1	29
C_1	+1	0.71
ω_1	+1	25
Response	Predicted values	Experimental values
Q_{deh}	25.636	25.71
COP_{hybrid}	2.209	2.21
\dot{M}	2.791	3.01

The optimized dehumidification performance of KCOOH solution was employed to examine the RSM model's ability to forecast the values of response parameters. Experiments conducted under optimized circumstances confirmed the optimal conditions. At optimal dehumidification performance, the response values were 25.636 (Q_{deh}), 2.209 (COP_{hybrid}), and 2.791 (\dot{M}). In contrast, the optimal dehumidification performance experimental values were 25.71 (Q_{deh}), 2.21 (COP_{hybrid}), and 3.01 (\dot{M}). Consequently, the experimental response results were consistent with the projected response values.

5. Comparison of Hybrid System with Conventional VCR Unit

The primary purpose of the proposed HLDAC system is to conserve energy from an electricity consumption standpoint and perform better than conventional VCS under

similar environmental conditions. Therefore, several experimental runs were performed to estimate the COP of a standalone VCR unit, and the COP was discovered to be 1.72. This lower value of COP (usually greater than 2.5) is due to the consideration of energy utilized by the electric heater and compressor in the system. They are employed to rewarm the cold airflow from the evaporator to a comfortable temperature. The comparison between the COP of hybrid systems and standalone systems is provided in Table 9. In addition to this comparison, Table 9 shows the distribution of the LHL by dehumidifier unit and the VCS unit discretely. The findings from Table 9 show that the value of COP_{hybrid} is greater than the COP of a conventional VCS. This is attributed to the remarkable LHL shared by the dehumidifier unit in an HLDAC system, in contrast to the added power consumed by the pump and blowers.

Table 9. Comparison of LHL shared and COP of hybrid system.

Experimental Run	COP_{hybrid}	LHL Shared by Dehumidifier (%)	LHL Shared by Evaporator (%)	Improvement (%)
1	1.85	40.54	59.46	7.56
2	1.86	41.67	58.33	8.13
3	1.79	33.73	66.27	4.07
4	1.75	25.42	74.58	1.74
5	2.18	53.01	46.99	26.74
6	2.14	52.65	47.35	24.41
7	1.98	49.53	50.47	15.12
8	1.86	41.55	58.45	8.13
9	1.84	39.99	60.01	6.97
10	1.85	40.57	59.43	7.56
11	1.79	34.01	65.99	4.07
12	1.76	28.41	71.59	2.32
13	2.21	55.21	44.79	28.48
14	2.17	52.03	47.97	26.16
15	1.99	51.01	48.99	15.69
16	1.87	41.87	58.13	8.72
17	1.88	42.67	57.33	9.31
18	1.81	36.89	63.11	5.23
19	1.93	43.86	56.14	12.21
20	1.8	34.78	65.22	4.65
21	1.78	32.98	67.02	3.48
22	2.01	51.89	48.11	16.86
23	1.81	37.75	62.25	5.23
24	1.83	39.31	60.69	6.39
25	1.82	38.81	61.19	5.81

Table 9 shows that in experimental run 13, the maximum value of 28.48% improvement in COP_{hybrid} is spotted; when both m_{a1} and T_{d1} are at lower values and C_1 and ω_1 are at high values. Additionally, it is self-evident that the LHL shared by the dehumidifier was found to be 55.21% by removing moisture from processed air. The reason behind the improved performance of the HLDAC system at lower air flow rates is that there is an increase in contact time between the processed air and desiccant, resulting in more MRR

than at higher air flow rates. Moreover, lower desiccant temperature enhances the capacity of the liquid desiccant to absorb more moisture content from incoming air due to enhanced driving force. At an optimal level of desiccant concentration, the tendency to provide effective dehumidification increases. Moreover, with the increasing humidity level of inlet air, the value of the dehumidifier's latent heat load will increase. The minimum increase in percent improvement in COP_{hybrid} (1.74%) is found during run 4, when T_{d1} and m_{a1} are at their maximum values and C_1 and ω_1 are at minimum values. The reason for the above is explained earlier. According to the data obtained, this is the least significant combination. In this configuration, the VCR unit's evaporator contributes approximately 74.58% of the LHL by lowering the temperature of incoming air to dew point. The temperature below dew point can be adjusted by the cut-off control employed in the VCR unit.

6. Economic Assessment

An energy-saving analysis was conducted for the proposed HLDAC system compared to that of a standalone VCS unit. Furthermore, 6 kW is the highest gross heat load covered by the HLDAC system. The operating conditions at this output were maximum values of m_{a1} , C_1 , ω_1 , and T_{d1} at its lowest value. In this operating condition, the energy-saving analysis is conducted.

In economic analysis of the hybrid system, all costs are taken into account, i.e., capital costs as well as operating costs of the proposed hybrid system. The total annual cost is comprised of investment cost (initial purchasing) (\dot{C}_{ic}) and operating cost (\dot{C}_{oc}). The \dot{C}_{ic} is divided into equal annual payments for the life span of the system (t years), and can be expressed as [44]:

$$\dot{C}_{ic}[\$/year] = \sum C_{cc} \times \varnothing \times \zeta \quad (24)$$

where C_{cc} , \varnothing , and ζ represent the component cost, maintenance factor, and cost recovery factor, respectively. The investment costs of components are given in Table 10. The cost recovery factor can be calculated by the expression [44]:

$$\zeta = \frac{i(1+i)^t}{(1+i)^t - 1} \quad (25)$$

Table 10. Investment cost of component of hybrid system.

Component	Investment Cost	Selection and Applicability of the Equations
SW-HX	$C_{SW-HX} = 100 \times (A_{SW-HX})^{0.6}$	Applicable for aluminum plate fine HE [45]
Pumps	$C_{pump} = 2100 \times \left(\frac{\dot{W}_{pump}}{10,000}\right)^{0.26} \times \left(\frac{1-\eta_p}{\eta_p}\right)^{0.5}$	Power law relations for single pass pump [46,47]
Condenser	$C_{Cond} = 8000 \times \left(\frac{A_{cond}}{100}\right)^{0.6}$	
AA-HX	$C_{AA-HX} = 8000 \times \left(\frac{A_{AA-HX}}{100}\right)^{0.6}$	
Compressor	$C_{comp} = \frac{39.5 \times \dot{m}_{ref}}{(0.9-\eta_{comp})}$	Applicable for fin based HE with area in range of 4.65–836 m ² [48]
Evaporator	$C_{evap} = 231 \times (A_{evap})^{0.693}$	
Expansion valve	$C_{exp} = 114.5 \times \dot{m}_{ref}$	
Dehumidifier/regenerator	$C_{deh} = C_{column} + C_{packing}$ $C_{column} = 583.6 \times H_{deh} \times d_{deh}^{0.675} \times \left(\frac{14.5 \times P_{atm}}{50}\right)^{0.44}$ $C_{packing} = C_{ppm} \times h_{deh} \times \frac{\pi \times d_{deh}^2}{4}$	Applicable for cylindrical packed towers with random Raschig rings for any column dimensions [49]

The annual operating cost can be expressed as:

$$\dot{C}_{oc} [\$/year] = ECA [kWh] \times C_{unit} \quad (26)$$

where $ECA [kWh]$ represents annual electricity consumption and C_{unit} is the electric cost per unit.

An energy-saving analysis was conducted for the proposed HLDAC system compared to that of a standalone VCS unit. Furthermore, 6 kW is the highest gross heat load covered by the HLDAC system. The operating conditions at this output were maximum values of m_{a1} , C_1 , ω_1 and T_{d1} at its lowest value. In this operating condition, the energy-saving analysis is conducted. The initial capital cost of the HLDAC system is INR 99,000, which includes the cost of a VCS unit and fabrication expenditure of the HLDAC system. The initial expenditure of a standalone 3.5 kW VCS with an electric heater arrangement for reheating was INR 48,000. Therefore, the extra expenditure (EE) is found to be INR 51,000; considering that the system works for 8 h per day for a whole month, i.e., 30 days, and assuming that the system maintains cooling load for eight months, taking into account India's average unit price of INR 6.15 per kWh [50]. The operating costs of the standalone VCS unit and the HLDAC system are found to be INR 53,136 and INR 35,424, respectively. Hence, the operating annual cost savings (OACS) are found to be INR 17,712. Moreover, considering a life span time of seven years for the HLDAC system and an interest rate of 10%, using these economic statistics, the payback period (PP) may be calculated as follows [51]:

$$PP = \frac{\ln\left(\frac{EE \times i}{OACS} + 1\right)}{\ln(i + 1)} \quad (27)$$

By performing the above calculations, the payback period is found to be 2.65 years. Table 11 summarizes the economic analysis of the proposed HLDAC system. Figure 8 shows the payback period of 2.65 years with total savings of INR 119,000 in the next 4.4 years.

Table 11. Economic assessment of HLDAC system compared to VCS unit.

Item	Value
Overall heat capacity of proposed system	6 kW
Capital investment of VCS unit with heater	INR 48,000
Capital investment of HLDAC system	INR 99,000
Extra Expenditure (ΔEE)	INR 51,000
Power consumed by VCS unit	3 kW
Power consumed by HLDAC system	2 kW
Average electric unit price	INR 6.15 per kWh
Annual operating cost of HLDAC system	INR 35,424
Annual operating cost of VCS unit	INR 53,136
Annual savings on electricity	INR 17,712R
Payback period (PP)	2.65 years

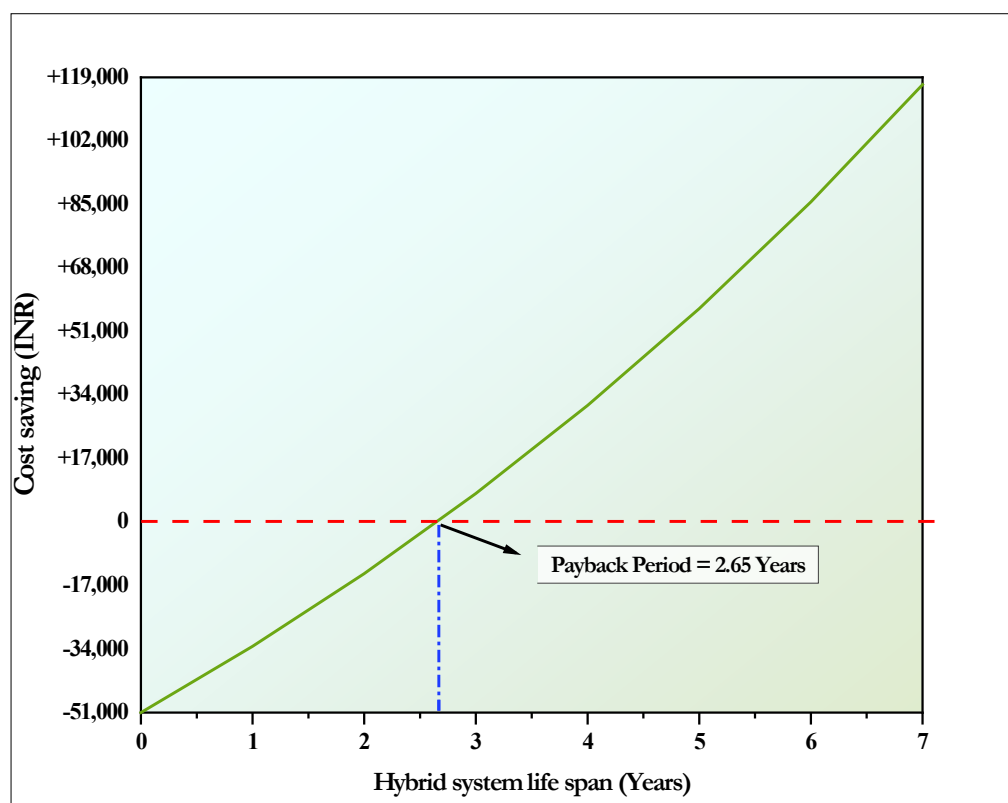


Figure 8. Payback period plot for HLDAC system.

7. Conclusions

This research experimentally examined a small-scale, 6 kW capacity HLDAC system, which was designed and developed by combining LDDS and a VCS unit. This research demonstrates that RSM is a convenient method to optimize the parameters of the dehumidification performance of KCOOH solution and analyze the relationship between input (independent) variables and response parameters. The following conclusions can be drawn:

- The maximum Q_{deh} and COP_{hybrid} is obtained when the values of specific air humidity and desiccant concentration are higher with the lowest values of air flow rate and desiccant temperature.
- Highest values of air flow rate, specific air humidity, desiccant concentration, and the lowest value of desiccant temperature yield maximum MRR.
- In the analysis of the results, it was observed that the effect of desiccant concentration has a greater effect on response variables as compared to other input variables.
- In terms of COP_{hybrid} , a 28.48% improvement is observed as compared to the standalone VCS. In this scenario, 55.21% of the LHL is shared by the dehumidifier unit.
- The proposed HLDAC system demands an additional initial investment of INR 51,000. However, this hybrid system saves INR 17,712 annually compared to a standalone VCS, with a payback time of 2.65 years assuming an interest rate of 10%.

Author Contributions: Conceptualization, K.K. and A.S.; methodology, K.K.; software, K.K.; validation, K.K.; data curation, K.K.; writing—original draft preparation, K.K.; writing—review and editing, A.S.; supervision, A.S.; funding acquisition, K.K. All authors have read and agreed to the published version of the manuscript.

Funding: This research received no external funding.

Institutional Review Board Statement: Not applicable.

Informed Consent Statement: Not applicable.

Data Availability Statement: The data presented in this study are available on request from the corresponding author.

Acknowledgments: We would like to extend our sincere gratitude and appreciation to the editors and anonymous reviewers for their comments and suggestions.

Conflicts of Interest: The authors declare no conflict of interest.

Nomenclature

A	Superficial air flow rate ($\text{kg}/\text{m}^2 \cdot \text{s}$)
a_t	Specific surface area of packing (m^2/m^3)
c_p	Isobaric specific heat ($\text{kJ}/\text{kg} \cdot \text{K}$)
COP_{hybrid}	Coefficient of performance of hybrid system
D	Superficial desiccant flow rate ($\text{kg}/\text{m}^2 \cdot \text{s}$)
ECA	Electricity consumption annually (kWh)
h_{fg}	Latent heat of evaporation (kJ/kg)
\dot{m}_a	Air flow rate (kg/s)
Δh_{abs}	Enthalpy of absorption (kJ/kg)
h	Enthalpy (kJ/kg)
H	Height (m)
h_{fg}	Latent heat of evaporation
Δh_{dil}	Enthalpy of dilution (kJ/kg)
i	Interest rate (%)
M	Molar mass (kg/kmol)
N_v	Molar vapor mass transfer flux ($\text{kmol}/\text{m}^2\text{s}$)
T	Temperature ($^{\circ}\text{C}$)
\dot{Q}	Heat load removal rate (kW)
Q	Heat load (kJ/kg)
C	Desiccant concentration ($\text{kg}_{\text{des}}/\text{kg}_{\text{sol}}$)
\dot{W}	Work transfer rate (W)
w	Specific air humidity (g/kg)
ω	Air humidity ratio ($\text{kg}/\text{kg}_{\text{da}}$)
Z	Height of dehumidifier/regenerator section

Greek letters

Δ	Difference or change in quantity
η	Efficiency
\emptyset	Maintenance factor
λ	Latent heat of condensation (kJ/kg)
ξ	Cost recovery factor

Subscripts

a	Air side
$AA - HX$	Air-air heat exchanger
cc	Component cost
ic	Investment cost
$cond$	Condenser
d	Desiccant side
deh	Dehumidifier
da	Dry air
exp	Expansion valve
l	Liquid phase
oc	Operating cost
p	Pump
ppm	Price of packing material
reg	regenerator
ref	reference

sol	Desiccant solution
SW – HX	Solution-water heat exchanger
<i>v</i>	Vapor phase
1	Inlet to dehumidifier
2	Exit of dehumidifier
3	Inlet of evaporator
4	Exit of evaporator

Abbreviations

AC	Air-conditioning
ANOVA	Analysis of variance
CCD	Central composite design
COP	Coefficient of performance
CaCl ₂	Calcium chloride
DOE	Design of experiments
HLDAC	Hybrid liquid desiccant air-conditioning
KCOOH	Potassium formate
LHL	Latent heat load
LDDS	Liquid desiccant dehumidification system
LDAC	Liquid desiccant air-conditioning
LiBr	Lithium bromide
LiCl	Lithium chloride
MgCl ₂	Magnesium chloride
MRR	Moisture removal rate
RSM	Response surface methodology
SSV	Sum of squares value
TEG	Triethylene glycol
TR	Tons of refrigeration
VCS	Vapor compression refrigeration system

References

- Calvino, F.; La Gennusa, M.; Rizzo, G.; Scaccianocce, G. The control of indoor thermal comfort conditions: Introducing a fuzzy adaptive controller. *Energy Build.* **2004**, *36*, 97–102. [[CrossRef](#)]
- Elnaklah, R.; Alnuaimi, A.; Alotaibi, B.S.; Topriska, E.; Walker, I.; Natarajan, S. Thermal comfort standards in the Middle East: Current and future challenges. *Build. Environ.* **2021**, *200*, 107899. [[CrossRef](#)]
- Santamouris, M.; Cartalis, C.; Synnefa, A.; Kolokotsa, D. On the impact of urban heat island and global warming on the power demand and electricity consumption of buildings—A review. *Energy Build.* **2015**, *98*, 119–124. [[CrossRef](#)]
- Ding, G. Recent developments in simulation techniques for vapour-compression refrigeration systems. *Int. J. Refrig.* **2007**, *30*, 1119–1133. [[CrossRef](#)]
- Zaki, O.M.; Mohammed, R.H.; Abdelaziz, O. Separate sensible and latent cooling technologies: A comprehensive review. *Energy Convers. Manag.* **2022**, *256*, 115380. [[CrossRef](#)]
- Jain, S.; Bansal, P.K. Performance analysis of liquid desiccant dehumidification systems. *Int. J. Refrig.* **2007**, *30*, 861–872. [[CrossRef](#)]
- Dai, Y.J.; Wang, R.Z.; Zhang, H.F.; Yu, J.D. Use of liquid desiccant cooling to improve the performance of vapor compression air conditioning. *Appl. Therm. Eng.* **2001**, *21*, 1185–1202. [[CrossRef](#)]
- Al-Farayedhi, A.; Gandhidasan, P.; Antar, M.A.; Gaffar, M.S.A. Experimental study of hybrid liquid desiccant based vapor compression cooling system. In Proceedings of the 6th Saudi Engineering Conference, KFUPM, Dhahran, Saudi Arabia, 14–17 December 2002; Volume 5, pp. 503–515.
- Lee, J.H.; Jeong, J.W. Hybrid heat-pump-driven liquid-desiccant system: Experimental performance analysis for residential air-conditioning applications. *Appl. Therm. Eng.* **2021**, *195*, 117236. [[CrossRef](#)]
- Guan, B.; Liu, X.; Zhang, Q.; Zhang, T. Performance of a temperature and humidity independent control air-conditioning system based on liquid desiccant for industrial environments. *Energy Build.* **2020**, *214*, 109869. [[CrossRef](#)]
- Mansuriya, K.; Raja, B.D.; Patel, V.K. Experimental assessment of a small scale hybrid liquid desiccant dehumidification incorporated vapor compression refrigeration system: An energy saving approach. *Appl. Therm. Eng.* **2020**, *174*, 115288. [[CrossRef](#)]
- Mansuriya, K.; Patel, V.K.; Raja, B.D.; Mudgal, A. Assessment of liquid desiccant dehumidification aided vapor-compression refrigeration system based on thermo-economic approach. *Appl. Therm. Eng.* **2020**, *164*, 114542. [[CrossRef](#)]
- Giampieri, A.; Ma, Z.; Ling-Chin, J.; Bao, H.; Smallbone, A.J.; Roskilly, A.P. Liquid desiccant dehumidification and regeneration process: Advancing correlations for moisture and enthalpy effectiveness. *Appl. Energy* **2022**, *314*, 118962. [[CrossRef](#)]
- Guan, B.; Zhang, T.; Liu, J.; Liu, X.; Yin, Y. Review of internally cooled liquid desiccant air dehumidification: Materials, components, systems, and performances. *Build. Environ.* **2022**, *211*, 108747. [[CrossRef](#)]

15. Ertas, A.; Anderson, E.E.; Kiris, I. Properties of a new liquid desiccant solution-Lithium chloride and calcium chloride mixture. *Sol. Energy* **1992**, *49*, 205–212. [[CrossRef](#)]
16. Fumo, N.; Goswami, D.Y. Study of an aqueous lithium chloride desiccant system: Air dehumidification and desiccant regeneration. *Sol. Energy* **2002**, *72*, 351–361. [[CrossRef](#)]
17. Salikandi, M.; Ranjbar, B.; Shir Khan, E.; Shanmuga Priya, S.; Thirunavukkarasu, I.; Sudhakar, K. Recent trends in liquid desiccant materials and cooling systems: Application, performance and regeneration characteristics. *J. Build. Eng.* **2021**, *33*, 101579. [[CrossRef](#)]
18. Kumar, M.; Mehla, N.; Srivastava, S.; Kant Ravi, R. Water generation from atmospheric air by using desiccant materials-nature-based solution-a review. *World J. Eng.* **2022**. [[CrossRef](#)]
19. Kumar, K.; Singh, A. Assessment of dehumidification performance of non-corrosive desiccant in hybrid liquid desiccant-vapour compression system. *Energy Sources Part A Recovery Util. Environ. Eff.* **2022**, *44*, 6909–6926. [[CrossRef](#)]
20. Longo, G.A.; Gasparella, A. Experimental analysis on chemical dehumidification of air by liquid desiccant and desiccant regeneration in a packed tower. *J. Sol. Energy Eng. Trans. ASME* **2004**, *126*, 587–591. [[CrossRef](#)]
21. Longo, G.A.; Gasparella, A. Experimental and theoretical analysis of heat and mass transfer in a packed column dehumidifier/regenerator with liquid desiccant. *Int. J. Heat Mass Transf.* **2005**, *48*, 5240–5254. [[CrossRef](#)]
22. Longo, G.A.; Fedele, L. Experimental measurement of equilibrium vapour pressure of H₂O/KCOOH (potassium formate) solution at high concentration. *Int. J. Refrig.* **2018**, *93*, 176–183. [[CrossRef](#)]
23. Wen, T.; Wang, M.; Chen, Y.; He, W.; Luo, Y. Thermal properties study and performance investigation of potassium formate solution in a falling film dehumidifier/regenerator. *Int. J. Heat Mass Transf.* **2019**, *134*, 131–142. [[CrossRef](#)]
24. Wen, T.; Luo, Y.; Sheng, L. Experimental study on the corrosion behavior and regeneration performance of KCOOH aqueous solution. *Sol. Energy* **2020**, *201*, 638–648. [[CrossRef](#)]
25. Zhang, X.; Wu, J.; Li, Z.; Chen, Y. A hybrid flue gas heat recovery system based on vapor compression refrigeration and liquid desiccant dehumidification. *Energy Convers. Manag.* **2019**, *195*, 157–166. [[CrossRef](#)]
26. Hong, J.K.; Hwang, I.; Roh, C.W.; Kim, M.S. Performance investigation on electro dialysis regeneration of potassium formate desiccant solution for liquid desiccant air-conditioning systems. *Energy Build.* **2022**, *266*, 112112. [[CrossRef](#)]
27. Cheng, X.; Yin, Y.; Guo, Y.; Zhou, W. Experimental study on a novel air conditioning system for deep cascade utilization of waste heat. *Appl. Therm. Eng.* **2022**, *200*, 117695. [[CrossRef](#)]
28. Chen, X.; Su, Y.; Aydin, D.; Bai, H.; Jarimi, H.; Zhang, X.; Riffat, S. Experimental investigation of a polymer hollow fibre integrated liquid desiccant dehumidification system with aqueous potassium formate solution. *Appl. Therm. Eng.* **2018**, *142*, 632–643. [[CrossRef](#)]
29. Kumar, K.; Singh, A.; Shaik, S.; Saleel, C.A.; Aabid, A.; Baig, M. Comparative Analysis on Dehumidification Performance of KCOOH–LiCl Hybrid Liquid Desiccant Air-Conditioning System: An Energy-Saving Approach. *Sustainability* **2022**, *14*, 3441. [[CrossRef](#)]
30. Elsarrag, E.; Ali, E.E.M.; Jain, S. Design guidelines and performance study on a structured packed liquid desiccant air-conditioning system. *HVAC R Res.* **2005**, *11*, 319–337. [[CrossRef](#)]
31. Mohtar, H.; Chesse, P.; Chalet, D. Describing uncertainties encountered during laboratory turbocharger compressor tests. *Exp. Tech.* **2017**, *36*, 53–61. [[CrossRef](#)]
32. Moffat, R.J. Describing the uncertainties in experimental results. *Exp. Therm. Fluid Sci.* **1988**, *1*, 3–17. [[CrossRef](#)]
33. Treybal, R.E.; Kulkarni, M.R. *Scilab Textbook Companion for Mass-Transfer Operations*; McGraw Hill Book Company: New York, NY, USA, 2013. Available online: <http://spoken-tutorial.org/NMEICT-Intro> (accessed on 20 October 2022).
34. Babakhani, D.; Soleymani, M. An analytical solution for air dehumidification by liquid desiccant in a packed column. *Int. Commun. Heat Mass Transf.* **2009**, *36*, 969–977. [[CrossRef](#)]
35. Liu, X.; Jiang, Y.; Xia, J.; Chang, X. Analytical solutions of coupled heat and mass transfer processes in liquid desiccant air dehumidifier/regenerator. *Energy Convers. Manag.* **2007**, *48*, 2221–2232. [[CrossRef](#)]
36. Weissman, S.A.; Anderson, N.G. Design of Experiments (DoE) and Process Optimization. A Review of Recent Publications. Available online: <https://pubs.acs.org/doi/abs/10.1021/op500169m> (accessed on 28 September 2022).
37. Khuri, A.I.; Mukhopadhyay, S. Response surface methodology. *Wiley Interdiscip. Rev. Comput. Stat.* **2010**, *2*, 128–149. [[CrossRef](#)]
38. Bhattacharya, S. Central Composite Design for Response Surface Methodology and Its Application in Pharmacy. In *Response Surface Methodology in Engineering Science*; IntechOpen: London, UK, 2021. [[CrossRef](#)]
39. Rafique, M.M.; Gandhidasan, P.; Bahaidarah, H.M.S. Liquid desiccant materials and dehumidifiers—A review. *Renew. Sustain. Energy Rev.* **2016**, *56*, 179–195. [[CrossRef](#)]
40. Mei, L.; Dai, Y.J. A technical review on use of liquid-desiccant dehumidification for air-conditioning application. *Renew. Sustain. Energy Rev.* **2008**, *12*, 662–689. [[CrossRef](#)]
41. Koronaki, I.P.; Christodoulaki, R.I.; Papaefthimiou, V.D.; Rogdakis, E.D. Thermodynamic analysis of a counter flow adiabatic dehumidifier with different liquid desiccant materials. *Appl. Therm. Eng.* **2013**, *50*, 361–373. [[CrossRef](#)]
42. Bassuoni, M.M. Experimental performance study of a proposed desiccant based air conditioning system. *J. Adv. Res.* **2014**, *5*, 87–95. [[CrossRef](#)]
43. Wen, T.; Luo, Y.; Wang, M.; She, X. Comparative study on the liquid desiccant dehumidification performance of lithium chloride and potassium formate. *Renew. Energy* **2021**, *167*, 841–852. [[CrossRef](#)]

44. Dixit, M.; Arora, A.; Kaushik, S.C. Thermodynamic and thermoeconomic analyses of two stage hybrid absorption compression refrigeration system. *Appl. Therm. Eng.* **2017**, *113*, 120–131. [[CrossRef](#)]
45. Xie, G.N.; Sunden, B.; Wang, Q.W. Optimization of compact heat exchangers by a genetic algorithm. *Appl. Therm. Eng.* **2008**, *28*, 895–906. [[CrossRef](#)]
46. Misra, R.D.; Sahoo, P.K.; Sahoo, S.; Gupta, A. Thermoeconomic optimization of a single effect water/LiBr vapour absorption refrigeration system. *Int. J. Refrig.* **2003**, *26*, 158–169. [[CrossRef](#)]
47. Garousi Farshi, L.; Mahmoudi, S.M.S.; Rosen, M.A. Exergoeconomic comparison of double effect and combined ejector-double effect absorption refrigeration systems. *Appl. Energy* **2013**, *103*, 700–711. [[CrossRef](#)]
48. Couper, J.R.; Penney, W.R.; Fair, J.R.; Walas, S.M. *Chemical Process Equipment: Selection and Design*; Gulf Professional Publishing: Hoboken, NJ, USA, 2009. Available online: [https://books.google.co.in/books?hl=en&lr=&id=IMkb4VBxqo4C&oi=fnd&pg=PR8&dq=J.R.+Couper,+W.R.+Penney,+J.R.+Fair,+Chemical+Process+Equipment-Selection+and+Design+\(Revised+2nd+Edition\),+Gulf+Professional+Publishing,+2009.&ots=4cR4c4dTE3&sig=-gK2qvNWYk866JpZyz0Nt0gdyGQ&redir_esc=y#v=onepage&q&f=false](https://books.google.co.in/books?hl=en&lr=&id=IMkb4VBxqo4C&oi=fnd&pg=PR8&dq=J.R.+Couper,+W.R.+Penney,+J.R.+Fair,+Chemical+Process+Equipment-Selection+and+Design+(Revised+2nd+Edition),+Gulf+Professional+Publishing,+2009.&ots=4cR4c4dTE3&sig=-gK2qvNWYk866JpZyz0Nt0gdyGQ&redir_esc=y#v=onepage&q&f=false) (accessed on 22 October 2022).
49. Brunazzi, E.; Nardini, G.; Paglianti, A. An Economical Criterion for Packed Absorption Column Design. *Chem. Biochem. Eng. Q.* **2002**, *15*, 199–206. Available online: https://www.researchgate.net/profile/Elisabetta-Brunazzi/publication/240625736_An_Economical_Criterion_for_Packed_Absorption_Column_Design/links/5660b63108aebae678aa3265/An-Economical-Criterion-for-Packed-Absorption-Column-Design.pdf (accessed on 26 October 2022).
50. Ghali, K. Energy savings potential of a hybrid desiccant dehumidification air conditioning system in Beirut. *Energy Convers. Manag.* **2008**, *49*, 3387–3390. [[CrossRef](#)]
51. Duffie, J.; Beckman, W. *Solar Engineering of Thermal Processes*; John Wiley & Sons: Hoboken, NJ, USA, 2013. Available online: <https://books.google.com/books?hl=en&lr=&id=Q1tjDQAAQBAJ&oi=fnd&pg=PR17&dq=+J.A.+Duffie&ots=ZkdThpjHNF&sig=ck2iXtuu2Aq04NV8llkd17hSpdU> (accessed on 3 August 2022).